# Speckle and Vibration

6.161 Final Project

Michael Mandel

December 17, 2003

## Abstract

This experiment explored the use of Electronic Speckle Pattern Interferometry and related speckle techniques to measure the vibrational modes of a circular membrane. In all, nine modes were photographed, the frequencies of which match the nine lowest vibrational modes of an ideal circular membrane, although the observed modal patterns did not.

# Contents



# List of Figures

# 1 Introduction

A CCD can record a hologram. The large size of the pixels greatly limits the possible resolution of such a hologram, but by exploiting the properties of coherent light impinging on rough surfaces one can create an electronic hologram. This technique is particularly well-suited to holographic interference measurements, a field known as Electronic Speckle Pattern Interferometry (ESPI).

Holographic interferometry can measure deformation due to applied loads and vibration. ESPI can measure the same properties of objects and more while having the additional benefits of being fast, cheap, and easy. It requires no lengthy or expensive development process and can even create movies in real time. The digital nature of the images allows further processing and synthesis of more than two images so that for example by varying the wavelength and phase of the light used one could reconstruct the 3D shape of an object accurate on the order of $1\mu m$.

This experiment used ESPI and related speckle techniques to measure the vibrational modes of a circular rubber membrane.

# 2 Approach

I will first introduce the concept of speckle, then analyze a system for measuring vibration using ESPI, and finally describe the concepts behind the system I used to make the photographs in Appendix A.

## 2.1 Speckle

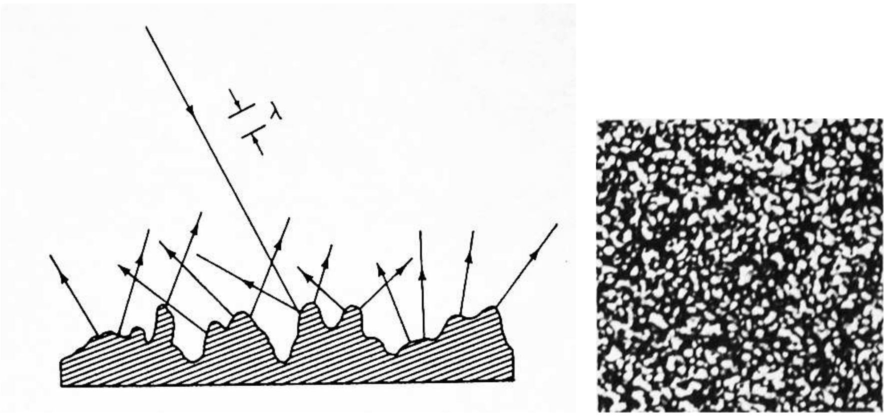


(a) A surface rough on the order of the wavelength.

(b) An example of speckle

**Figure 1: Taken from [Gåsvik 95]**

Coherent light falling on a surface that is rough on the order of the wavelength of the light (see Figure 1(a)) and approximated as Lambertian will be scattered by that surface in all directions and at all phases uniformly distributed between 0 and $2\pi$. When this light is imaged, its intensity forms a random field of light and dark "speckles," (see Figure 1(b)) the size of which are determined by the aperture of the imaging lens.

To find the field at any given position in the image, consider all of the light that gets focused to that point as infinitesimally short phasors added together. Assuming the phases are uniformly distributed and that all of the amplitudes and phases are independent of each other, this phasor addition becomes a random walk through the complex plane starting at the origin. The statistics of such random walks render the real and imaginary parts of the complex field independent, zero-mean, identically distributed Gaussian random variables, with the intensity distributed according to a negative exponential as seen in Figure 2. [Goodman 76]

$$Pr(I) = \begin{cases} \frac{1}{\bar{I}}\exp(\frac{-I}{\bar{I}}) & I \geq 0 \\ 0 & otherwise \end{cases} \tag{1}$$

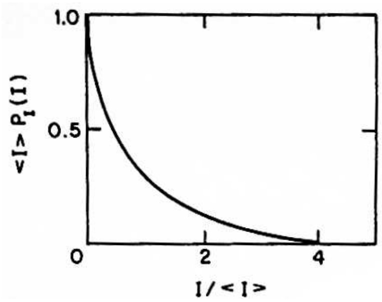


**Figure 2: Probability density function of a polarized speckle pattern [Goodman 76].**

## 2.2 ESPI

When a speckle pattern object beam

$$U_o(\vec{x}) = u_o(\vec{x})e^{j\phi_o(\vec{x})} \tag{2}$$

meets a smooth, collimated reference beam

$$U_r(\vec{x}) = u_r(\vec{x})e^{j\phi_r(\vec{x})} \tag{3}$$

the intensity is given by

$$I_1(\vec{x}) = u_o^2 + u_r^2 + 2u_o u_r \cos(\phi_o - \phi_r) \tag{4}$$

where I have left off the $(\vec{x})$ from the $u$s and $\phi$s for clarity. If the surface creating the speckle is vibrating, it induces a phase shift in the object beam by an amount

$$\Delta\phi(\vec{x}, t) = \Delta\phi_o \cos(\omega t) \tag{5}$$

so that the intensity at a given point in a given instant is

$$I_2(\vec{x}, t) = u_o^2 + u_r^2 + 2u_o u_r \cos(\phi_o - \phi_r - \Delta\phi_o \cos(\omega t)) \tag{6}$$

Assuming that the object is vibrating much more quickly than the frame rate of the camera (i.e. $2\pi\omega = \frac{1}{\tau} \gg 30$ Hz), the intensity at a pixel in the camera is averaged over many cycles, giving

$$I_c(\vec{x}) = \langle I_c(\vec{x}, t)\rangle_\tau = u_o^2 + u_r^2 + \frac{2u_o u_r}{\tau}\int_\tau \cos(\phi_o - \phi_r + \Delta\phi_o \cos(\omega t))dt \tag{7}$$

which can be evaluated to give

$$\langle I_c\rangle_\tau = u_o^2 + u_r^2 + 2u_o u_r \cos(\phi_o - \phi_r)J_0(\Delta\phi_o) \tag{8}$$

where $J_0(x)$ is the zero-order Bessel function.[Wykes 82]

The Bessel function has maxima and minima at $x = 0, 3.8, 7.0, 10.2, \ldots$, causing the speckle pattern to have maximal contrast, and has zeros at $x = 2.4, 5.5, 8.6, 11.8, \ldots$, causing the speckle to have minimal contrast. Thus, to visualize these differences in contrast one can high-pass filter and rectify the image, transforming differences in contrast to differences in mean brightness. The resulting image will have patterns of light and dark fringes, representing contours of equal vibrational amplitude. Since the Bessel function is not periodic, however, these fringes will not be spaced a fixed amplitude apart. The Bessel function's decaying envelope means that the zero-th order fringe will be brightest, with higher orders appropriately dimmer.[Wykes 82]

### 2.3 Final Approach

In order to be able to discern the above fringes, each fringe must be $\sim 5$ speckles wide. In order for the speckles to remain larger than the pixels of the camera, vibrational amplitudes must remain small to prevent the fringes from disappearing. As amplitudes grow beyond this point, however, macroscopic movements in the surface tend to blur the speckles together. Nodes in the standing wave patterns in the specific structure under inspection keep the speckle stationary and speckle contrast high. Thus one may subtract the image of the stationary structure from that of the vibrating structure and everything that remains the same (i.e. the nodes of the standing wave pattern) will cancel, while the moving parts will not cancel. The resultant image will then have light spots where the structure is moving and dark spots where it is still, sacrificing sensitivity for range of measurement. This technique also has the advantage of not requiring a reference beam and thus having a much simpler setup.

## 3 Experimental Procedures

Both of these setups shine coherent laser light from a 500 mW $Ar^+$ laser on a vibrating rubber membrane, built by taping a latex glove around another roll of tape. The membrane's vibration is driven by a small speaker placed behind it, which is powered a signal generator playing sinusoids of varying frequency and amplitude. Images are captured by the IMAQ image capture tool and analyzed off line with a simple Matlab script shown in Figure 3. See also Figure 4 for an example of the use of this script. At first I used the ESPI setup described below, but after realizing the ineffectualness of the reference beam I switched to the second, simpler setup.

```
function im = fringes(im1, im2)
% subtracts the two images and low pass filters to find the fringes
% in the speckle.

im = abs(double(im1) - double(im2));
lpf = fspecial('gaussian', 4, .7);
im = imfilter(im, lpf);
imagesc(im);
```

**Figure 3: Matlab code for processing images. Takes as arguments a reference image of the stationary setup and an image of the moving membrane.**

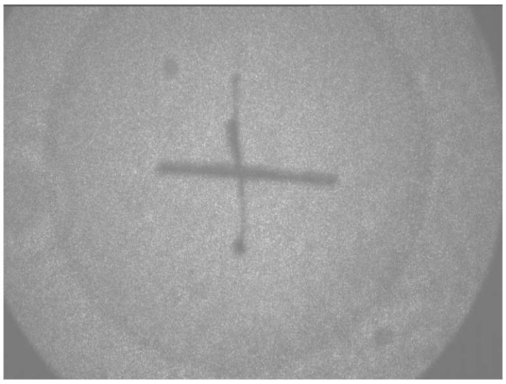

(a) Membrane photographed with no sound playing

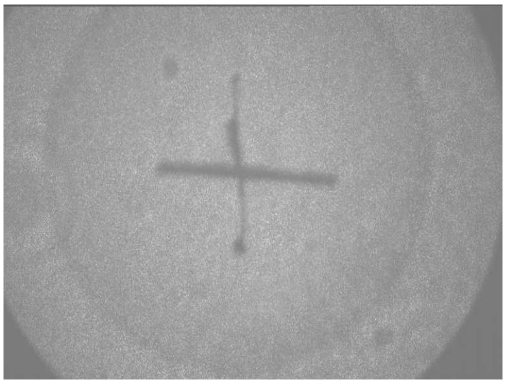

(b) Membrane photographed with 675 Hz tone playing

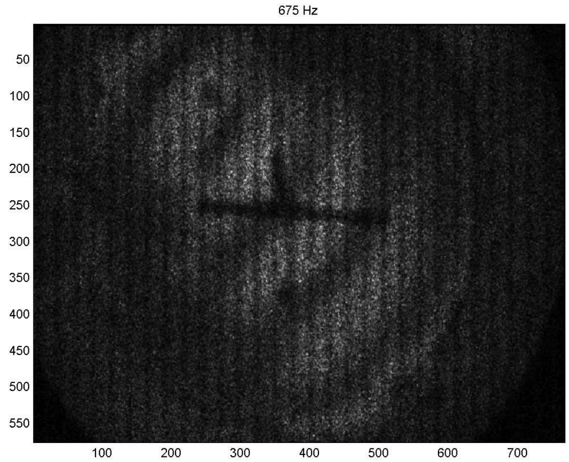


(c) Fringes formed by processing 4(a) and 4(b) with Matlab code in Figure 3

**Figure 4: Example of Matlab processing of two images to view the membrane's vibrational pattern at 675 Hz.**

## 3.1 ESPI Setup

ESPI interferes a reference beam with the image of the speckle reflected from the target. See Figure 5(a) for a schematic. The laser light is first split by a variable beam-splitter into object and reference beams. The reference beam is expanded and spatially filtered before shining on the CCD through another beam splitter. The object beam is expanded and spatially filtered before shining on the target, which creates the speckle pattern. The speckle pattern in then imaged by the lens and aperture bouncing off the second beam splitter and onto the CCD.

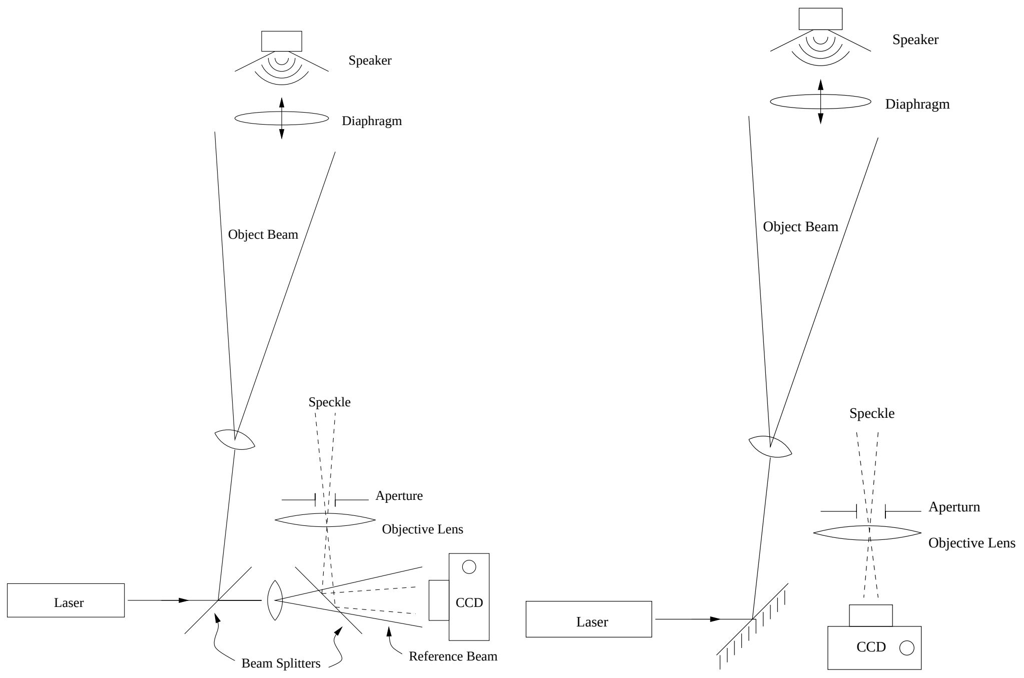


(a) ESPI setup, note the presence of a reference beam.

(b) Final setup, photographing speckle pattern directly

**Figure 5: Comparison of the two setups used in this experiment.**

## 3.2 Final Setup

This configuration simply photographs the speckle pattern on the moving membrane. See Figure 5(b) for a schematic and Figure 6 for a photograph. This time, the laser light is reflected from a full mirror, through a beam expander and spatial filter onto the target. The speckle pattern is then imaged by the aperture-lens system directly onto the CCD camera.

This setup has the nice characteristic that the speckle blurring due to vibration is visible to the naked eye (perhaps more visible through the tiny hole in the middle of a hooked finger). In order to photograph the modes, then, I adjusted the driving frequency until I saw a pattern and then took a number of pictures at varying amplitudes. A real time system would have allowed a more complete search for the vibrational modes of the membrane, as it was sometimes difficult to determine when I was looking at one pattern or a superposition of two patterns.

## 3.3 Other Experimental Parameters

In addition to the two setups described above, I examined a number of fringe-finding techniques and targets until I found a combination that actually produced fringes.

[Doval 00] and [Wykes 82] list image subtraction, image addition, and manipulations of a single image as methods for extracting fringes from vibrating membranes. Of the subtraction methods, one can subtract adjacent frames or subtract the same reference frame from each subsequent frame. My eventual elimination of the reference beam and dependence on motion blur required me to subtract a reference image from the images of driven oscillation. High pass filtering and rectification of a single driven image produced fringes with very low contrast on my data, and addition did not

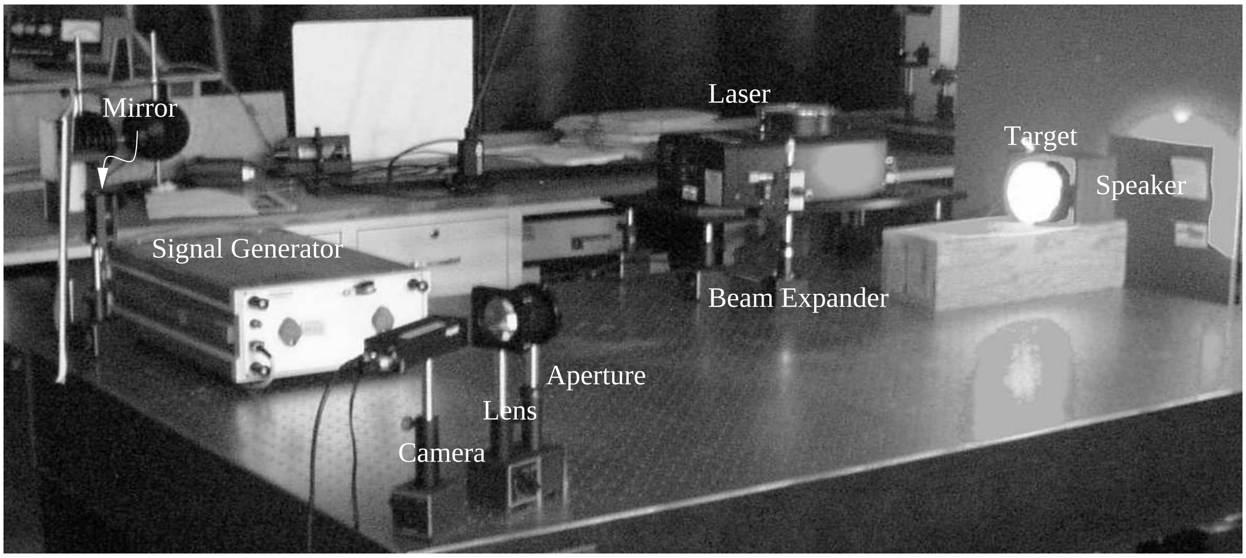


**Figure 6: A photograph of the final setup**

create fringes at all.

The initial goal of this experiment was to find the vibrational modes of a speaker cone or cabinet. Both of these absorb light well, and so do not produce much speckle without a very bright laser. Furthermore, the speaker cone vibrates far too much for any of it to remain stationary, as required by this measurement technique. Measuring a piece of paper taped to a 1.5 inch diameter, only the (0,1) mode was observable. A piece of paper taped to a rectangular frame might have worked, but after a few attempts I decided its modes would be too hard to analyze.

# 4 Experimental Results and Analysis

Sweeping through all frequencies from 200 Hz to 1000 Hz, I managed to identify nine oscillatory modes of the rubber membrane. See Appendix A for photographs of all of them from lowest frequency to highest. Observation of the mode patterns indicates that the nine modes I have found are not the first nine, however aligning the modal frequencies, the observed modes match the first nine frequencies of an ideal membrane well, as can be seen in Table 4 and Figure 7.

One possible explanation is that these aren't circular harmonics at all, but somewhere between rectangular and circular because of nonuniform tension around the rim of the membrane. This hypothesis is supported by the simultaneous presence of the obviously circular mode at 490 Hz seen in Figure 10 and the orthogonal (3,1) modes at 530 and 675 Hz seen in Figures 11 and 13. The proximity of observations to theory also might indicate that the this technique does not image the modal patterns as I would expect it to, rendering my modal observations invalid and supporting the claim that I have found the lowest nine modes.

# 5 Conclusions

The final measurement system successfully photographed nine vibrational patterns in the circular rubber membrane. It is less clear which modes these photographs represent, judging from the frequencies at which they occur.

**Table 1: Comparison of ideal modes and frequencies to those observed. Mode designations are of the form (d,c) where d is the number of nodal diameters and c is the number of nodal circles. Frequencies are measured relative to the ideal fundamental, assuming that the observed fourth mode is the ideal fourth mode. Ideal mode information taken from [Tabla 99].**

| Ideal Freq | Ideal Mode | Observed Freq | Observed Mode |
|---|---|---|---|
| 1.000 | (0,1) | 1.085 | (1,1) |
| 1.594 | (1,1) | 1.519 | (2,1) |
| 2.136 | (2,1) | 2.126 | (3,0) |
| 2.296 | (0,2) | 2.300 | (3,1) |
| 2.653 | (3,1) | 2.699 | (3,2) |
| 2.918 | (1,2) | 2.929 | (3,1) |
| 3.156 | (4,1) | 3.081 | (4,2) |
| 3.501 | (2,2) | 3.298 | (4,3) |
| 3.600 | (0,3) | 4.209 | (5,2) |

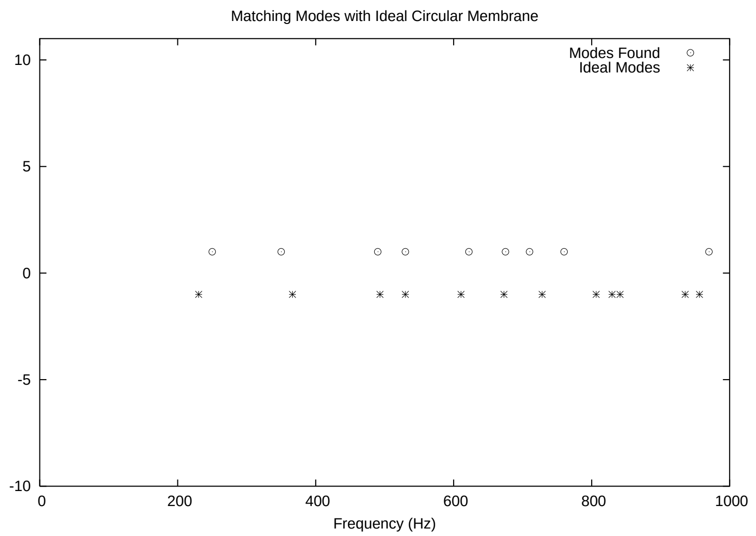


**Figure 7: Matching measured modes of the membrane to those of an ideal membrane assuming that the fourth measured mode is actually the fourth ideal mode.**

## 5.1 Further Work

In general, the most room for improvement in this experiment lies in the target. Ideally, one would use a circular metal plate clamped around the edges and driven mechanically so as to drastically reduce the observed amplitude. Were one to use such a metal plate, one could again try the ESPI setup. In the same vein, the target should be prevented from moving as a whole, so as to further increase sensitivity.

The improvement that would have helped the most in this particular application of speckle metrology would have been a real-time system capable of showing the current mode. Such a system would have made identifying and isolating vibrational modes trivial because they would all have been clearly visible on the computer screen. The investigator would not have to search by eye for a suitable pattern before taking pictures for verification.

This experiment could also be improved by more precise measurements. Using an oscillating mirror, one could modulate the reference beam at the same frequency as the vibration (homodyne) or slightly above or below it (heterodyne) so that the fringes appear frozen, or move slowly through the phase relationships, respectively [Doval 00]. Using a pulsed laser or a frame rate faster than the vibration frequency, one could freeze the object and accurately measure amplitudes by subtracting successive frames.

## References

[Chen 98] Chen, Fang, Christopher Griffen, T E Allen. "Digital Speckle Interferometry: Some Developments and Applications for Vibration Measurement in the Automotive Industry." Opt Eng Vol 37, No 5, pp1390-1397 (May 1998).

[Dixon 98] Dixon, G J. "Speckle Techniques Map Deformation and Displacement." Laser Focus World, pp75-78, June 1998.

[Doval 00] Doval, Ángel. "A Systematic Approach to TV Holography." Meas Sci Tech Vol 11 (2000), R1-R36.

[Gåsvik 95] Gåsvik, Kjell. *Optical Metrology.* Chichester: John Wiley and Sons, 1995.

[Goodman 76] Goodman, Joseph. "Some Fundamental Properties of Speckle." JOSA, Voll 66, No 11, pp1145-1150 (November 1976).

[Goodman 85] Goodman, Joseph. "A Random Walk Through the Field of Speckle." SPIE Vol 556, Int'l Conference on Speckle (1985).

[Sjödahl 98] Sjödahl, M. "Some Recent Advances in Electronic Speckle Photography." Optics and Lasers in Engineering, Vol 29 (1998).

[Tabla 99] Tabla.com. "Acoustical Properties of Drums and the Tabla." http://www.tabla.com/tablaph1.html (1999)

[Wykes 82] Wykes, Catherine. "Use of Electronic Speckle Pattern Interferometry (ESPI) in the Measurement of Static and Dynamic Surface Displacements." Optical Engineering, May/June 1982, Vol 21 No 3.

# A Appendix: Photographs

N.B.: in these pictures a cross appears in the middle of the membrane and vertical lines run throughout. The cross I drew on the membrane to facilitate focusing the camera. The vertical lines are an artifact of the CCD, as they were present in every image, even unfocused ones. Also, mode designations are of the form (d,c) where d is the number of nodal diameters and c is the number of nodal circles.

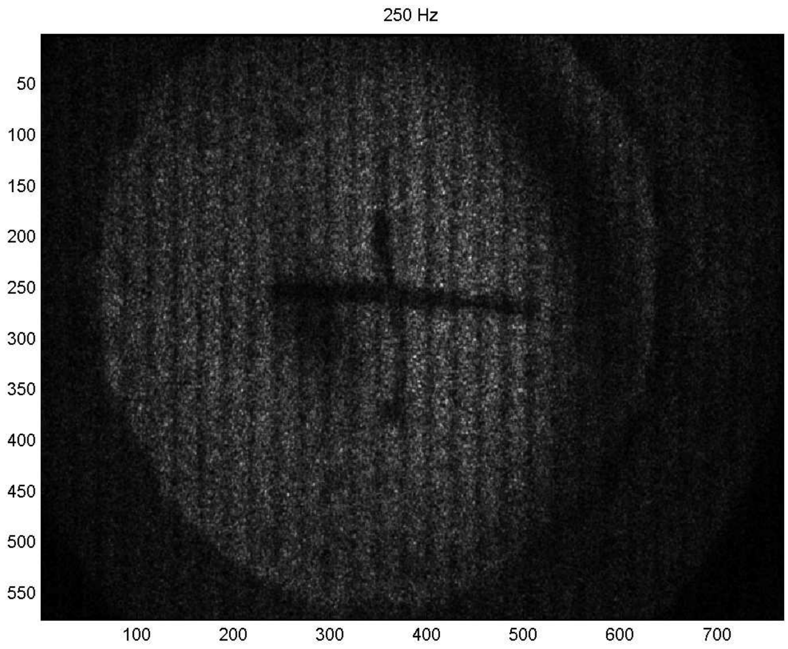


**Figure 8: 250 Hz, (1,1) Mode**

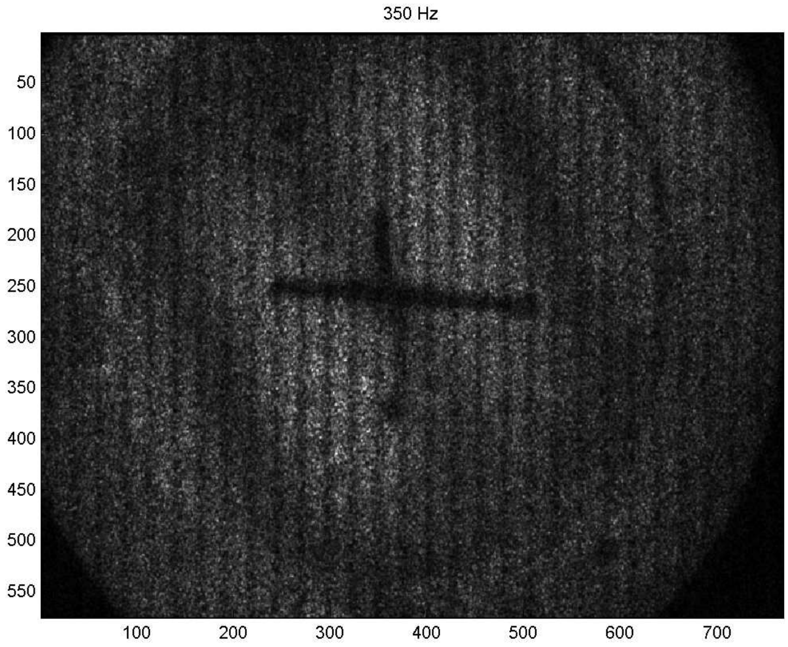


**Figure 9: 350 Hz, (2,1) Mode**

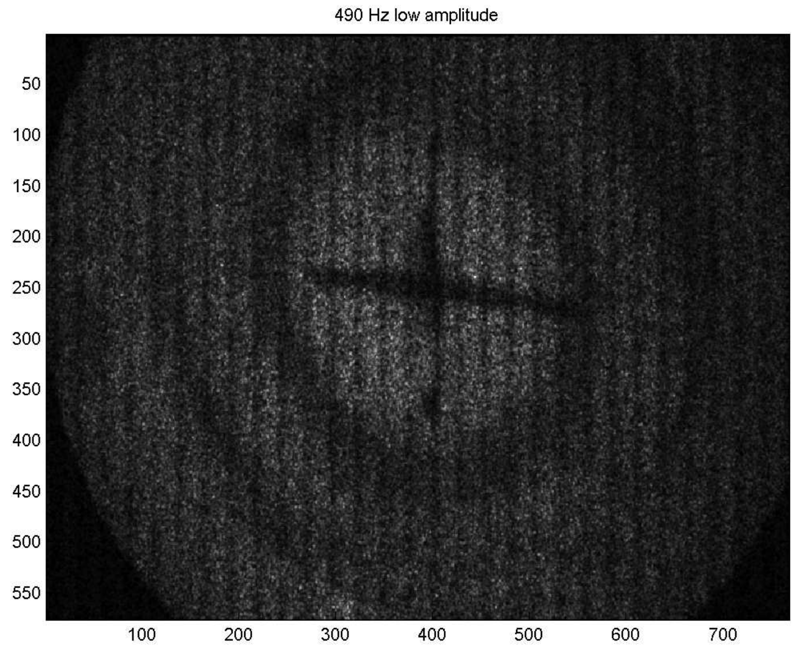


**Figure 10: 490 Hz, (3,0) Mode**

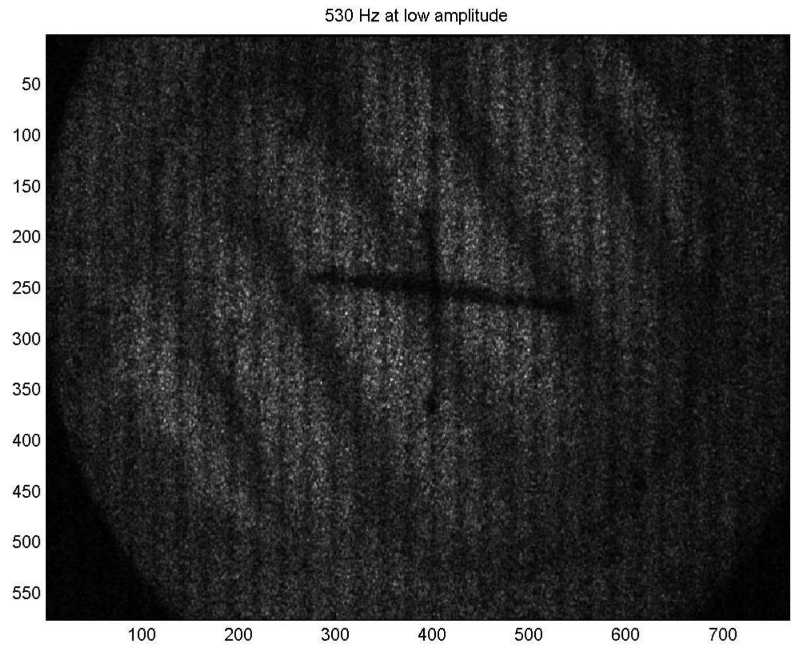


**Figure 11: 530 Hz, (3,1) Mode**

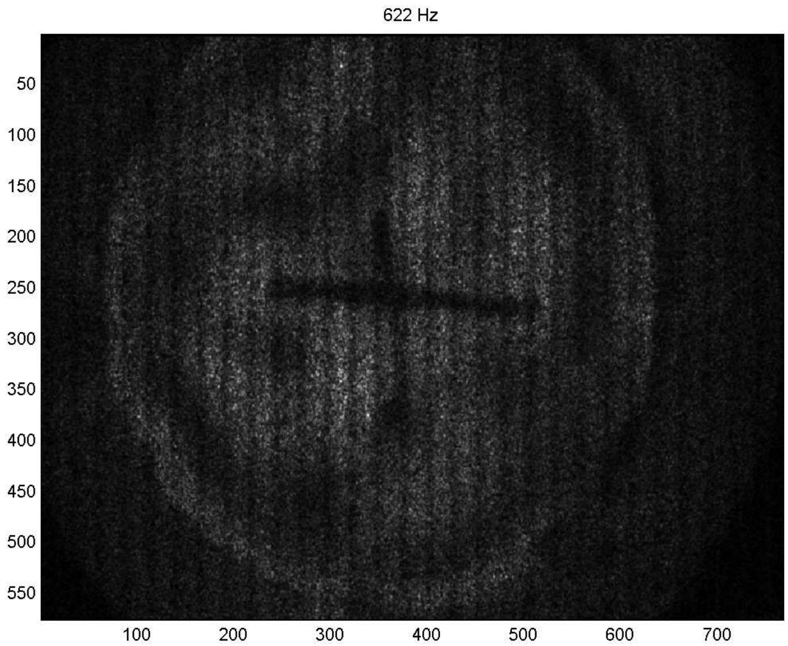


**Figure 12: 622 Hz, (3,2) Mode**

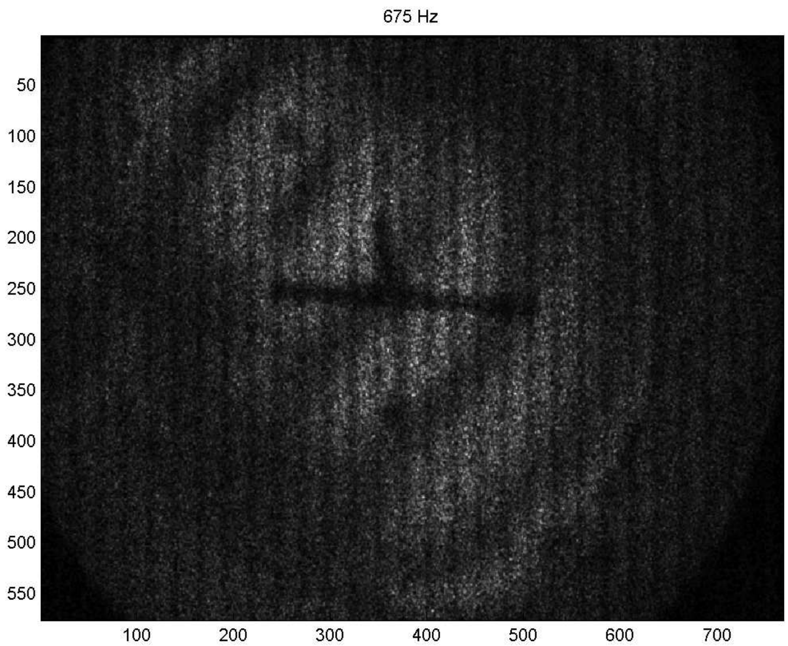


**Figure 13: 675 Hz, (3,1) Mode**

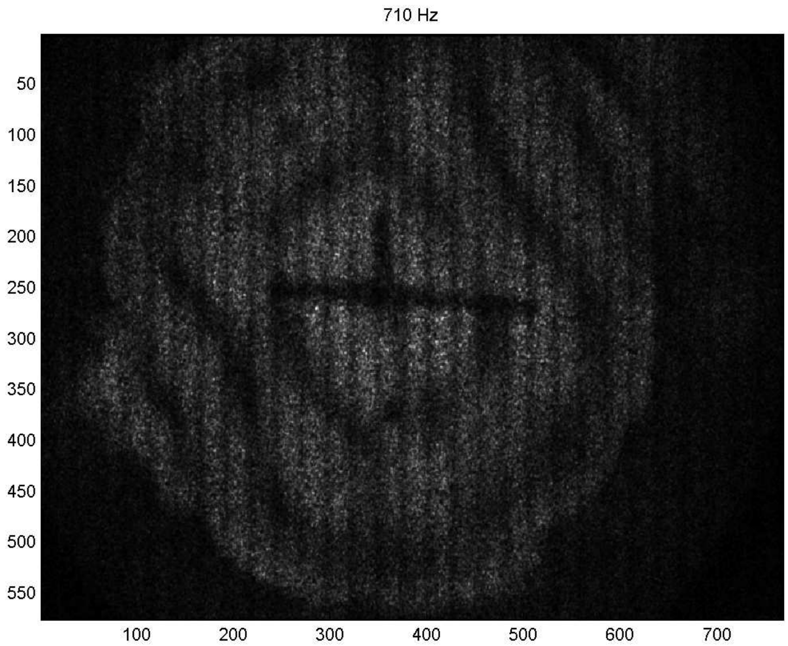


**Figure 14: 710 Hz, (4,2) Mode**

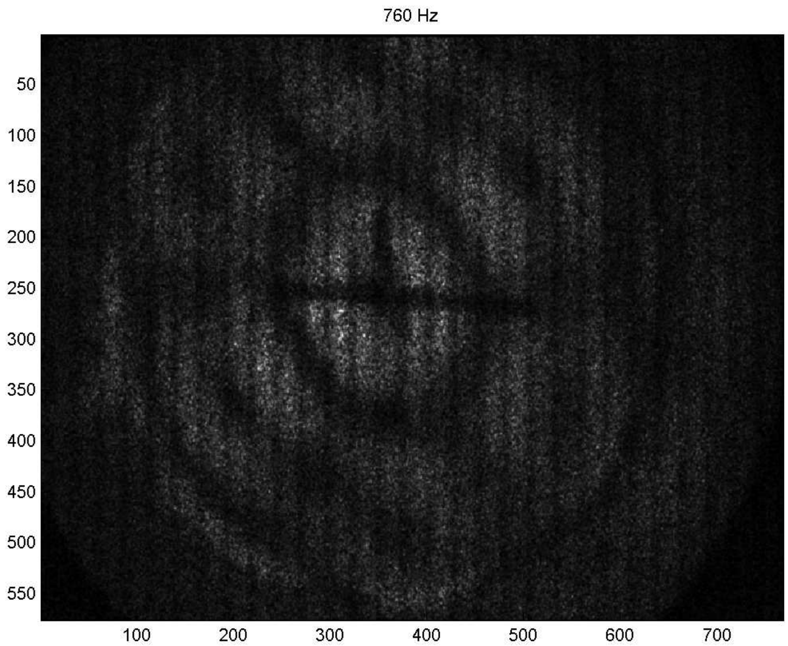


**Figure 15: 760 Hz, (4,3) Mode**

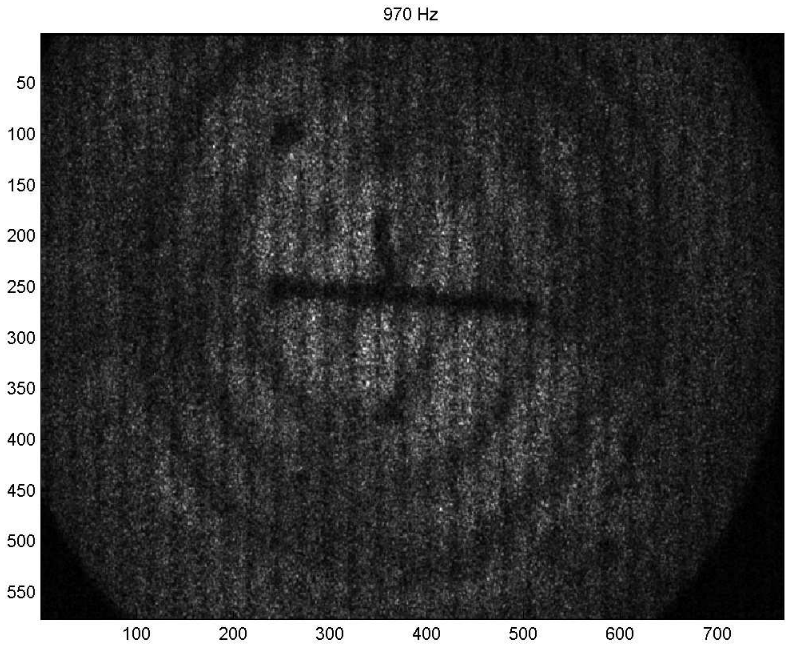


**Figure 16: 970 Hz, (5,2) Mode**